

# A graphical Gaussian process model for multi-fidelity emulation of expensive computer codes

Yi Ji<sup>1</sup>, Simon Mak<sup>1</sup>, Derek Soeder<sup>2</sup>, J-F Paquet<sup>2</sup>, and Steffen A. Bass<sup>2</sup>

<sup>1</sup>Department of Statistical Science, Duke University

<sup>2</sup>Department of Physics, Duke University

## Abstract

We present a novel Graphical Multi-fidelity Gaussian Process (GMGP) model that uses a directed acyclic graph to model dependencies between multi-fidelity simulation codes. The proposed model is an extension of the Kennedy-O’Hagan model for problems where different codes cannot be ranked in a sequence from lowest to highest fidelity.

## 1 Introduction

With recent breakthroughs in scientific computing, computer simulations are quickly replacing physical experiments in many modern physics and engineering problems. These simulations allow scientists to better understand complex physical systems which may be prohibitively expensive or infeasible for direct experimentation. This shift to computer experimentation has found success in a variety of exciting applications, including rocket design [9] and universe expansions [7]. These computer experiments, however, can demand a hefty price in computational resources, requiring thousands or millions of CPU hours per experiment. One way to address this is via surrogate modeling (or emulation): a handful of simulations is first run at carefully chosen design points, then a “surrogate” model is fit to efficiently predict the expensive computer code. A popular choice of surrogate model is the Gaussian process (GP) [12], which allows for closed-form expressions for prediction and uncertainty quantification.

As systems become more realistic and complex, computer experiments become increasingly more expensive to perform; in such cases, the simulation data needed to train an accurate emulator can be difficult to obtain. One solution is *multi-fidelity emulation*. The idea is to collect data from the “high-fidelity” simulator, which is computationally expensive but provides a detailed representation of model physics, as well as data from “lower-fidelity” simulators, which make simplifying assumptions on model physics but can be performed quickly. With this data, a multi-fidelity emulator is trained to predict output from the high-fidelity simulator. The key advantage is that, by leveraging information from low-fidelity data to enhance predictions for the high-fidelity model, one can train an accurate emulator using much fewer high-fidelity training data (and thereby lower computational costs). The development of such a multi-fidelity emulator

model is an active research area. A widely-used model is the Kennedy-O’Hagan (KO) model [8], which models a sequence of computer codes (from lowest to highest fidelity) using a sequence of GP models linked by a linear autoregressive framework. [5] proposed a recursive formulation of the KO model to allow for more efficient computation. [11] further generalized this model via a non-linear autoregressive framework, which allows for more flexible correlation structures via a deep GP formulation.

There is a key limitation of these existing methods: they presume the multi-fidelity nature of computer codes forms a sequence from lowest to highest fidelity. This may not be the case for complex physics problems. Take, e.g., the heavy-ion collision framework in [4] for simulating the quark-gluon plasma, which filled the universe prior to the formation of matter. This simulation consists of three stages: the initial energy disposition of colliding nuclei, the hydrodynamic evolution of plasma, and the conversion of nuclear fluid into particles. At each stage  $m$ , a physicist can choose one of  $N_m > 1$  models (some more accurate but time-consuming, others less accurate but quick), resulting in  $N_1 N_2 N_3$  combinations of simulation codes. In such a problem, it is difficult to rank the different simulation codes in a sequence from lowest to highest fidelity, since some codes may be more accurate for one stage but less accurate for another. Hence, to apply existing methods, one may have to ignore data from certain simulators or impose an artificial ordering to the codes, both of which may lead to significant increases in emulation error.

To address this, we present a new Graphical Multi-fidelity Gaussian Process (GMGP) model, which uses a directed acyclic graph (DAG) to model dependencies between computer codes. This DAG structure can often be derived from an inspection of the physics model. The GMGP integrates this DAG structure in the form of a Bayesian network within the GP surrogate model, which allows for a structured pooling of information from low-fidelity simulations to better predict the high-fidelity code. Section 2 provides background and motivation. Section 3 presents the GMGP modeling framework and recursive formulation. Section 4 discusses several methodological developments. Section 5 shows the effectiveness of the GMGP model over existing methods in a comprehensive numerical study. Section 6 concludes the paper.

## 2 Background & motivation

### 2.1 Gaussian process surrogate modeling

The Gaussian process model is a widely-used Bayesian non-parametric framework for predictive modeling. Let  $\mathbf{x} \in \mathbb{R}^d$  be the inputs for the computer code, and  $Z(\mathbf{x})$  be the corresponding computer code output. A GP surrogate model places the following prior on computer code  $Z$ :

$$Z(\cdot) \sim \mathcal{GP}(m(\cdot), k_{\boldsymbol{\theta}}(\cdot, \cdot)),$$

where  $m(\cdot)$  is the mean function and  $k_{\boldsymbol{\theta}}(\cdot, \cdot)$  is the covariance function with parameters  $\boldsymbol{\theta}$ . A typical choice of  $m(\cdot)$  is constant mean, and common choices for  $k_{\boldsymbol{\theta}}(\cdot, \cdot)$  include the squared exponential and Matérn kernels.

Suppose that the simulator is run at inputs  $\mathbf{D} = \{\mathbf{x}_1, \dots, \mathbf{x}_n\}$ , yielding simulation outputs  $\mathbf{z} =$

$\{Z(\mathbf{x}_1), \dots, Z(\mathbf{x}_n)\}$ . Without loss of generality, we fit a zero-mean GP regression on data. Conditional on  $\mathbf{D}$  and  $\mathbf{z}$ , the predictive distribution of the computer code  $Z$  at a new input point  $\mathbf{x}_*$  is given by:

$$Z(\mathbf{x}_*)|\mathbf{z}, \mathbf{D} \sim \mathcal{N}(\mu(\mathbf{x}_*), \sigma^2(\mathbf{x}_*)), \quad \mu(\mathbf{x}_*) = k(\mathbf{x}_*, \mathbf{D})K(\mathbf{D})^{-1}\mathbf{z}, \quad \sigma^2(\mathbf{x}_*) = k(\mathbf{x}_*, \mathbf{x}_*) - k(\mathbf{x}_*, \mathbf{D})K(\mathbf{D})^{-1}k(\mathbf{x}_*, \mathbf{D})^T,$$

where  $k(\mathbf{x}_*, \mathbf{D}) = [k(\mathbf{x}_*, \mathbf{x}_1), \dots, k(\mathbf{x}_*, \mathbf{x}_n)]$  and  $K(\mathbf{D})$  is the covariance matrix for the training data.

## 2.2 The Kennedy-O’Hagan model

A popular model for multi-fidelity emulation is the Kennedy-O’Hagan model [8], which models a sequence of computer codes with increasing fidelity via a sequence of linear autoregressive GP models. Let  $\{\mathbf{z}_1, \mathbf{z}_2, \dots, \mathbf{z}_T\}$  denote training data generated by  $T$  levels of code sorted in increasing accuracy, where  $\mathbf{z}_t = \{Z_t(\mathbf{x}_i^t)\}_{i=1}^{n_t}$  is the data from the  $t$ -th code  $Z_t$ . The KO model assumes the following multi-fidelity framework:

$$Z_t(\mathbf{x}) = \rho_{t-1} \cdot Z_{t-1}(\mathbf{x}) + \delta_t(\mathbf{x}), \quad Z_{t-1}(\mathbf{x}) \perp \delta_t(\mathbf{x}), \quad t = 2, \dots, T. \quad (1)$$

Here, the first code is assigned a GP prior  $Z_1(\mathbf{x}) \sim \mathcal{GP}(\mathbf{h}_1(\mathbf{x})^T \boldsymbol{\beta}_1, \sigma_1^2 r_1(\mathbf{x}, \mathbf{x}'))$ , and subsequent discrepancy terms are also assigned GP priors  $\delta_t(\mathbf{x}) \sim \mathcal{GP}(\mathbf{h}_t(\mathbf{x})^T \boldsymbol{\beta}_t, \sigma_t^2 r_t(\mathbf{x}, \mathbf{x}'))$ . In words, Equation (1) presumes that, prior to data, the code  $Z_t(\mathbf{x})$  can be decomposed as the lower-fidelity code  $Z_{t-1}(\mathbf{x})$  times a correlation parameter  $\rho_{t-1}$ , plus some discrepancy function  $\delta_t(\mathbf{x})$  which models systematic bias between the two codes.

A key development in the KO model is the recursive formulation proposed by [5], which allows for efficient emulator training. The key idea is to replace the GP prior  $Z_{t-1}(\mathbf{x})$  in Equation (1) by the *posterior* distribution  $Z_{t-1}^*(\mathbf{x}) = [Z_{t-1}(\mathbf{x})|\mathbf{z}_1, \dots, \mathbf{z}_{t-1}]$ , which can be shown to follow a GP. This recursive formulation decouples the original KO model into  $T$  GP regressions, which can greatly reduce computational cost for model training by avoiding the inversion of large ill-conditioned covariance matrices. With a nested structure for design points and noiseless observations, it can be shown in [5] that this recursive formulation yields the same posterior predictive mean and variance as the original KO model.

One limitation of the KO model (and its extensions) is that it presumes the computer codes form a sequence from lowest to highest fidelity. Consider a motivating example where this is not the case. We take the  $d = 20$ -dimensional test function from [13] as the high-fidelity code, and generate four lower-fidelity representations (details of this experiment are provided in Section 5). The dependence between these codes is captured in the DAG in Figure 1a: the two medium-fidelity codes ( $M_1$  and  $M_2$ ) are obtained via different simplifications on the high-fidelity code ( $H$ ), and the two low-fidelity codes ( $L_1$  and  $L_2$ ) are obtained by different averaging operations on  $M_1$ . This mimics the scenario where there are two different lower-fidelity approximations to  $H$ , and two different lower-fidelity approximations to  $M_1$ . Here, the KO model is unable to capture the underlying multi-fidelity framework, since the five codes cannot be ranked in a path from lowest to highest fidelity. One way to apply the KO model, which we adopt below, is to train it on data along the longest path  $L_1, M_1, H$  (see Figure 1a).

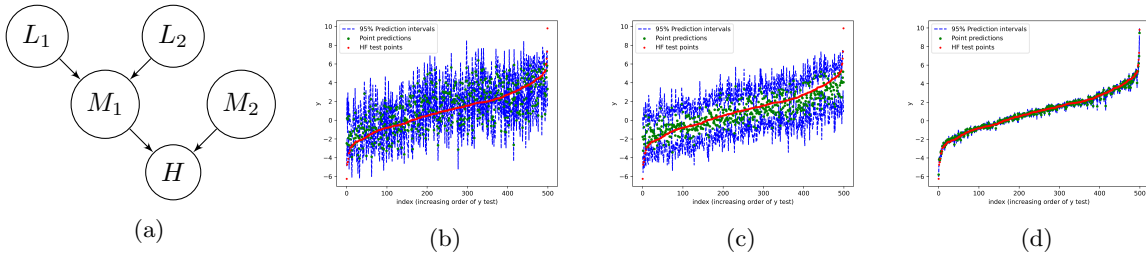


Figure 1: (a) DAG used in numerical study. (b)-(d) Predictions (green), 95% predictive intervals (blue) and the true high-fidelity output (red) for (b) the standard GP emulator, (c) the (recursive) KO emulator, and (d) the proposed (deep) GMGP model.

Figure 1c shows the predictive performance of the fitted KO model, compared to a standard GP model trained on only high-fidelity data (Figure 1b). We see that the KO model indeed improves predictive performance compared to a standard GP emulator. However, the fitted model with KO still has poor predictions and high uncertainty in many regions of the input space. A natural question to ask is whether, by integrating data from the two remaining codes ( $L_2$  and  $M_2$ ) in a principled fashion, we can improve predictions and reduce uncertainty for the emulator. Figure 1d answers this in the affirmative for the proposed model: by integrating data within a multi-fidelity DAG framework, the GMGP model yields much better predictive performance over the KO model. We describe this model in the following section.

### 3 The Graphical Multi-fidelity Gaussian Process model

#### 3.1 Model specification

We now present the proposed GMGP model, which generalizes the KO model by integrating DAG dependencies between codes within the GP model. Let  $V$  be the set of nodes representing different computer codes, and let  $T = |V| \in V$  be the node for the highest-fidelity code. Let  $E$  be the set of directed edges connecting different codes, where an edge between nodes  $t'$  and  $t$  is drawn *only* if the code at  $t$  is a *higher-fidelity refinement* of the code at  $t'$ . Let  $\mathcal{G} = (V, E)$  be the DAG for this multi-fidelity framework. This DAG structure can often be derived from an inspection of the underlying physics for the simulation models.

Let  $Z_t(\mathbf{x})$  be the computer code evaluated at input  $\mathbf{x}$ ,  $t \in V$ . The GMGP assumes the following model:

$$\begin{cases} Z_t(\mathbf{x}) = \sum_{t' \in \text{Pa}(t)} \rho_{t'}(\mathbf{x}) Z_{t'}(\mathbf{x}) + \delta_t(\mathbf{x}), & t \in \overline{V_S}, \\ Z_{t'}(\mathbf{x}) \perp \delta_t(\mathbf{x}), & t' \in \text{Pa}(t). \end{cases} \quad (2)$$

Here,  $V_S \subset V$  consists of all source nodes in  $\mathcal{G}$ ,  $\overline{V_S} = V \setminus V_S$  contains the remaining nodes, and  $\text{Pa}(t) = \{t' \in V : (t', t) \in E\}$  consists of all *parent* nodes of  $t \in V$  in the DAG  $\mathcal{G}$ . We further adopt the following GP priors on the code on source nodes:

$$\begin{cases} Z_t(\mathbf{x}) \sim \mathcal{GP}(\mathbf{h}_t(\mathbf{x})^T \boldsymbol{\beta}_t, \sigma_t^2 r_t(\mathbf{x}, \mathbf{x}')), & t \in V_S \\ Z_t(\mathbf{x}) \perp Z_{t'}(\mathbf{x}), & t, t' \in V_S, \quad t \neq t', \end{cases} \quad (3)$$

as well as independent GP priors on discrepancies  $\delta_t(\mathbf{x}) \sim \mathcal{GP}(\mathbf{h}_t(\mathbf{x})^T \boldsymbol{\beta}_t, \sigma_t^2 r_t(\mathbf{x}, \mathbf{x}')), t \in \overline{V_S}$ .

While the above specification may seem quite involved, the intuition is straight-forward. Note that, for every non-source node  $j \in \overline{V_S}$  in the DAG, its parent nodes  $\text{Pa}(j)$  contain all lower-fidelity models that are correlated with code  $j$ . Equation (2) therefore presumes that, prior to data, the code  $Z_t(\mathbf{x})$  can be decomposed as the weighted sum of its parent (lower-fidelity) codes, plus a discrepancy term  $\delta_t(\mathbf{x})$  to model systematic bias. The key novelty over the KO model is that, instead of pooling information in a line from lowest to highest fidelity, the GMGP can integrate information over a more general DAG structure, which better captures dependencies between codes in complex systems. By leveraging this graphical structure guided by simulation models, the GMGP can enjoy improved predictive performance over the KO model.

The GMGP framework provides two appealing modeling properties for multi-fidelity emulation, outlined in the proposition below.

**Proposition 1.** *The GMGP model defined above satisfies the following Markov properties:*

$$(a) Z_t(\mathbf{x}) \perp Z_{t'}(\mathbf{x}) | \{Z_j(\mathbf{x})\}_{j \in \text{Pa}(t)}, \quad \forall t' \notin \text{Des}(t) \cup \text{Pa}(t) \cup \{t\}$$

$$(b) Z_t(\mathbf{x}) \perp Z_{t'}(\mathbf{x}') | \{Z_j(\mathbf{x})\}_{j \in \text{Pa}(t)}, \quad \forall t' \in \text{Pa}(t), \quad \forall \mathbf{x}' \neq \mathbf{x}$$

where  $\text{Des}(t)$  denotes the set of descendant nodes for  $t$ ,  $t \in V$ .

Property (a) states that, for a given node  $t$ , the code output  $Z_t(\mathbf{x})$  and any code output  $Z_{t'}(\mathbf{x})$  (where  $t'$  is non-descendant, non-parent node of  $t$ ) are conditionally independent, given its parent nodes  $\{Z_j(\mathbf{x})\}_{j \in \text{Pa}(t)}$ . In other words, given knowledge of the code at its immediate *lower-fidelity* (i.e., *parent*) nodes  $\text{Pa}(t)$ , the output at any code which is not a *high-fidelity refinement* (i.e., not a *descendant*) of  $t$  yields no additional information on predicting the code  $Z_t(\mathbf{x})$  at node  $t$ . This is an intuitive property when directed edges in  $\mathcal{G}$  represent higher-fidelity refinement of codes (as specified earlier). Property (b) states that, for a given node  $t$ , the code output for a fixed input  $\mathbf{x}$   $Z_t(\mathbf{x})$  is conditionally independent of the output  $Z_{t'}(\mathbf{x}')$  for parent nodes at a different input  $\mathbf{x}'$ , given its parent nodes  $\{Z_j(\mathbf{x})\}_{j \in \text{Pa}(t)}$ . In other words, given knowledge of the code at its lower-fidelity (parent) nodes  $\text{Pa}(t)$  with input  $\mathbf{x}$ , the output of such codes at any other inputs  $\mathbf{x}'$  yields no additional information on predicting the code  $Z_t(\mathbf{x})$  at node  $t$ . This extends the Markov property provided in [10], which was used to justify the KO model.

Suppose the parameters  $\boldsymbol{\beta}$ ,  $\boldsymbol{\sigma}^2$ ,  $\boldsymbol{\rho}$  are fixed (these can be estimated via maximum likelihood). Conditional on simulation data  $\mathbf{z}^{(T)} = \{\mathbf{z}_1, \mathbf{z}_2, \dots, \mathbf{z}_T\}$ , where  $\mathbf{z}_t = \{Z_t(\mathbf{x}_i^t)\}_{i=1}^{n_t}$  are the observed outputs for the  $t$ -th code, the predictive distribution for the highest-fidelity code is given by  $[Z_T(\mathbf{x}) | Z^{(T)} = \mathbf{z}^{(T)}] \sim \mathcal{N}(m_{Z_T}(\mathbf{x}), s_{Z_T}^2(\mathbf{x}))$ , where:

$$m_{Z_T}(\mathbf{x}) = \left[ \sum_{t' \in \text{Pa}(T)} \rho_{t'}(\mathbf{x}) \mathbf{h}_{t'}(\mathbf{x})^T \boldsymbol{\beta}_{t'} + \mathbf{h}_T(\mathbf{x})^T \boldsymbol{\beta}_T \right] + \mathbf{t}_T(\mathbf{x})^T V_T^{-1} (\mathbf{z}^{(T)} - H_T \boldsymbol{\beta})$$

$$s_{Z_T}^2(\mathbf{x}) = v_{Z_T}^2(\mathbf{x}) - \mathbf{t}_T(\mathbf{x})^T V_T^{-1} \mathbf{t}_T(\mathbf{x}). \quad (4)$$

Here,  $\mathbf{t}_T(\mathbf{x}) = \text{Cov}(Z_T(\mathbf{x}), \mathbf{z}^{(T)})$ ,  $V_T$  is the covariance matrix of  $\mathbf{z}^{(T)}$ ,  $v_{Z_T}^2(\mathbf{x})$  is the prior variance of  $Z_T(\mathbf{x})$ , and  $H_T$  is the experience matrix of  $\mathbf{z}^{(T)}$  such that  $H_T \boldsymbol{\beta}$  gives the vector of prior means for  $\mathbf{z}^{(T)}$ . While

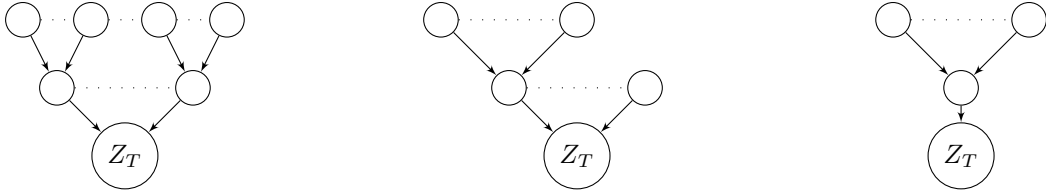


Figure 2: Examples of in-trees, with  $Z_T$  denoting the highest-fidelity code at the root.

Equation (4) provides closed-form expressions for the predictive distribution, these expressions can be unwieldy to compute due to the inverse of matrix  $V_T$ , which has dimensions  $\sum_{t=1}^{|T|} n_t \times \sum_{t=1}^{|T|} n_t$ . Motivated by [5], we consider below a recursive formulation of the GMGP model which decouples this inverse over the DAG, enabling efficient and scalable prediction from the GMGP.

### 3.2 Recursive formulation

We now present a recursive formulation of the GMGP model (or the r-GMGP model) in the spirit of [5], which allows for efficient training and prediction. The idea is to split the DAG into separate sub-graphs, perform training and prediction on each sub-graph, then combine this information over  $\mathcal{G}$  to obtain the full prediction. To do so, we need to make the following assumption on the multi-fidelity DAG structure  $\mathcal{G}$ . Suppose  $\mathcal{G}$  is an *in-tree* [6] (or *anti-arborescence tree*), defined as a tree in which one node (the highest-fidelity code) is designated as the “root”, and there exists exactly one path connecting any other node to  $T$ . Figure 2 shows several examples of in-trees. Such trees capture the multi-fidelity structure of a wide range of simulation problems.

With this in-tree structure, we now define the following recursive formulation of the GMGP:

$$\begin{cases} Z_t(\mathbf{x}) = \sum_{t' \in \text{Pa}(t)} \rho_{t'}(\mathbf{x}) Z_{t'}^*(\mathbf{x}) + \delta_t(\mathbf{x}), & t \in \overline{V_S} \\ Z_{t'}^*(\mathbf{x}) \perp \delta_t(\mathbf{x}), & t' \in \text{Pa}(t) \end{cases} \quad (5)$$

where  $Z_{t'}^*(\cdot) = [Z_{t'}(\cdot) | \{Z_m = \mathbf{z}_m\}_{m \in \text{Pa}(t')}]$  is the *posterior* distribution of the code at node  $t'$ , conditional on data from its immediate lower-fidelity (parent) nodes. The key difference between the r-GMGP model (5) and the GMGP model (2) is that the prior for the parent code  $Z_{t'}(\mathbf{x})$  is replaced by its posterior  $Z_{t'}^*(\mathbf{x})$ . This reformulation enables a recursive computation of predictive distribution from the leaves of  $\mathcal{G}$  to its root.

Under (5), the posterior distribution of the highest-fidelity code  $Z_T$  can be shown to be  $[Z_T(\mathbf{x}) | Z^{(T)} = \mathbf{z}^{(T)}] \sim \mathcal{N}(\mu_{Z_T}(\mathbf{x}), \sigma_{Z_T}^2(\mathbf{x}))$ , with the posterior mean and variance:

$$\begin{aligned} \mu_{Z_T}(\mathbf{x}) &= \left[ \sum_{t' \in \text{Pa}(T)} \rho_{t'}(\mathbf{x}) \mu_{Z_{t'}}(\mathbf{x}) + \mathbf{h}_T(\mathbf{x})^T \boldsymbol{\beta}_T \right] + r_T(\mathbf{x}, D_T)^T R_T(D_T)^{-1} \left[ \mathbf{z}_T - \sum_{t' \in \text{Pa}(T)} \rho_{t'}(D_T) \odot \mathbf{z}_{t'}(D_T) - \mathbf{h}_T(D_T)^T \boldsymbol{\beta}_T \right] \\ \sigma_{Z_T}^2(\mathbf{x}) &= \sum_{t' \in \text{Pa}(T)} \rho_{t'}^2(\mathbf{x}) \sigma_{Z_{t'}}^2(\mathbf{x}) + \sigma_T^2 \left[ 1 - r_T(\mathbf{x}, D_T)^T R_T(D_T)^{-1} r_T(\mathbf{x}, D_T) \right]. \end{aligned} \quad (6)$$

Here,  $\odot$  denotes the Hadamard (entrywise) product,  $r_T(\mathbf{x}, D_T)$  is the correlation vector between  $Z_T(\mathbf{x})$  and  $\mathbf{z}_T$ , and  $R_T(D_T)$  is the correlation matrix of  $\mathbf{z}_T$ . Equation (6) shows that the desired posterior distribution can be computed recursively on sub-graphs from the leaves of  $\mathcal{G}$  to its root, thereby avoiding inversion of the

large covariance matrix  $V_T$  for all observations  $\mathbf{z}^{(T)}$ .

The following proposition shows that the recursive equations in (6) indeed give the same predictive distribution as the original GMGP model:

**Proposition 2.** *Let  $\mathcal{G} = (V, E)$  be the considered multi-fidelity DAG, and suppose  $\mathcal{G}$  forms an in-tree. Further suppose the design points are nested over DAG  $\mathcal{G}$ , such that for any node  $t \in V$ , its design points  $D_t$  is a subset of the designs at all parent nodes  $D_{t'}$ ,  $t' \in \text{Pa}(t)$ . Then the posterior predictive mean and variance from the GMGP and r-GMGP models are the same, i.e.,  $m_{Z_T}(\mathbf{x}) = \mu_{Z_T}(\mathbf{x})$  and  $s_{Z_T}^2(\mathbf{x}) = \sigma_{Z_T}^2(\mathbf{x})$ .*

This proposition shows that the recursive GMGP model indeed yields the same predictive distribution as the original GMGP model, and does so at a much lower computational cost via recursion on sub-graphs.

## 4 Methodological Developments

We now discuss several methodological developments concerning experimental design and a more flexible formulation using deep GPs.

### 4.1 Experimental design over DAG

From Proposition 2, one desirable property of the experimental design is that points are *nested* over the DAG  $\mathcal{G}$ , meaning the design points for any node should be a subset of the design points of its parents in  $\mathcal{G}$ . To achieve this, we propose a bottom-up approach for such a nested experimental design on DAG  $\mathcal{G}$ . Here, we assume that there is only one highest-fidelity root node that we aim to predict, namely node  $T$ . The key idea is to first generate a space-filling (e.g., maximin) sliced Latin hypercube design (SLHD, [1]), where the number of design points in each slice equals the desired sample size on the root node  $T$ . The design points from the SLHD are then allocated to each node, starting from the root node  $T$  then filling out nodes sequentially via a breadth-first traversal of  $\mathcal{G}$  from the root. Algorithm 1 provides the detailed steps.

---

#### Algorithm 1 Nested Experimental Design on a DAG

---

- 1: Fix sample size at root node  $T$  to  $n$ . Suppose the sample size at other nodes are always multiple of  $n$ .
  - 2: Count total number of nodes in the graph, denoted by  $N$ . From bottom to top, number the nodes as Node 1, Node 2, ..., Node  $N$ . i.e., Node 1 is the root node and Node  $N$  is a source node.
  - 3: Apply SLHD [1] to generate  $M$ ,  $M \geq N$  slices of design points, each slice containing  $n$  samples.
  - 4: Assign design points in first  $N$  slices to the corresponding nodes on the DAG. i.e., Initially, Node  $i$  contains design points of Slice  $i$ , denoted as  $S_i = \{i\}$ ,  $i = 1, 2, \dots, N$ .
  - 5: Assign the remaining  $(M - N)$  slices to nodes where larger sample size is affordable and update  $S_i$ ,  $i > 1$ .
  - 6: Keep  $S_1$  unchanged. For Node  $i$ ,  $i = 2, 3, \dots, N$ , append the union of design points of descendant nodes of  $i$  to the design points at Node  $i$ . In other words,  $S_i = \{i\} \cup [\cup_{j \in \text{Des}(i)} S_j]$ .
-

## 4.2 Deep GMGP

One potential limitation of the GMGP (and r-GMGP) model is that it presumes a linear correlation structure between codes. In reality, the correlation between codes is likely nonlinear in nature, and a more complex surrogate model which integrates this nonlinear structure may be preferable given enough data. We present below a “deep-GMGP” (d-GMGP) model which incorporates such structure via deep GPs.

As before, suppose the multi-fidelity DAG  $\mathcal{G}$  is an in-tree, with design points nested over  $\mathcal{G}$ . The d-GMGP model can be formulated as follows:

$$\begin{cases} Z_t(\mathbf{x}) = f_t(\{Z_{t'}(\mathbf{x}) : t' \in \text{Pa}(t)\}) + \delta_t(\mathbf{x}), & t \in \overline{V_S} \\ f_t(\cdot) \perp \delta_t(\cdot) \end{cases} \quad (7)$$

where the discrepancies again follow GP prior  $\delta_t(\mathbf{x}) \sim \mathcal{GP}(0, \sigma_t^2 r_t(\mathbf{x}, \mathbf{x}'))$ , and the source nodes follow priors:

$$\begin{cases} Z_t(\mathbf{x}) \sim \mathcal{GP}(0, \sigma_t^2 r_t(\mathbf{x}, \mathbf{x}')), & t \in V_S \\ Z_t(\mathbf{x}) \perp Z_{t'}(\mathbf{x}), & t, t' \in V_S, \quad t \neq t', \end{cases} \quad (8)$$

The key difference between this model with the GMGP model (2) is that, instead of taking the weighted sum  $\sum_{t' \in \text{Pa}(t)} \rho_{t'}(\mathbf{x}) Z_{t'}(\mathbf{x})$  of the lower-fidelity parent codes, we allow for a more general (nonlinear) transformation  $f_t$  of  $\{Z_{t'}(\mathbf{x}) : t' \in \text{Pa}(t)\}$ . Since this transformation is unknown in practice, we can assign GP priors  $f_t \sim \mathcal{GP}(0, K_t(\cdot, \cdot))$ ,  $t \in \overline{V_S}$ . This nested modeling framework can be seen as a specific case of the deep GP model in [3], constrained by the underlying multi-fidelity DAG structure.

Inspired by [11], a recursive formulation can similarly be adopted for d-GMGP. The key idea is again to split the full  $\mathcal{G}$  and sequentially train each sub-graph along the DAG. As before, this is achieved by replacing the GP priors  $Z_{t'}(\cdot)$  in Equation (7) by the GP posteriors  $Z_{t'}^*(\cdot) = [Z_{t'}(\cdot) | \{Z_m = \mathbf{z}_m\}_{m \in \text{Pa}(t')}]$ . This recursive formulation of d-GMGP has the additional benefit of bypassing the complex variational approximations needed to fit the underlying deep GP model, thereby enabling efficient and scalable prediction.

The predictive methodology is similar to [11]. We first fit independent GP models on the source nodes (which represent the lowest-fidelity simulations), with  $r_t$  chosen to be an anisotropic Gaussian kernel. Next, we compute the posterior predictive mean functions at these nodes and evaluate them at design points of their child nodes. These posterior predictive means are then used as additional inputs for the child nodes. Following [11] and [2], a GP model is fit on  $f_t(\cdot)$  with kernel:

$$K_t = K_{\text{Gaussian}}(\mathbf{x}, \mathbf{x}') \cdot \left[ K_{\text{Linear}}(\mathbf{z}_{t'}^*(\mathbf{x}), \mathbf{z}_{t'}^*(\mathbf{x}')) + \prod_{t' \in \{\text{Pa}(t)\}} K_{\text{Gaussian}}(\mathbf{z}_{t'}^*(\mathbf{x}), \mathbf{z}_{t'}^*(\mathbf{x}')) \right] + K_{\text{Gaussian}}(\mathbf{x}, \mathbf{x}')$$

Here  $K_{\text{Linear}}(\mathbf{x}, \mathbf{x}') = v \mathbf{x}^T \mathbf{x}'$  with  $v$  as the variance parameter,  $\mathbf{z}_{t'}^*(\mathbf{x}) = \{Z_{t'}^*(\mathbf{x})\}_{t' \in \text{Pa}(t)}$  and we apply anisotropic Gaussian kernels for the rest. After the highest-fidelity code  $Z_T$  is trained, the posterior predictive mean and variance can then be computed via Monte Carlo integration. These Monte Carlo samples are

generated from the posterior distributions at each lower-fidelity model and propagated as inputs to higher-fidelity models.

## 5 Numerical Experiments

We now investigate the performance of the d-GMGP model compared to existing multi-fidelity models in a numerical experiment. In this test, we consider the same DAG shown in Figure 1a, which consists of two low-fidelity codes ( $L_1$  and  $L_2$ ), two medium-fidelity codes ( $M_1$  and  $M_2$ ) and one high-fidelity code ( $H$ ).

The high-fidelity code  $H$  is taken to be the  $d = 20$ -dimensional test function in [13]:

$$Z_H(\mathbf{x}) = \frac{5x_{12}}{1+x_1} + 5(x_4 - x_{20})^2 + x_5 + 40x_{19}^3 - 5x_{19} + 0.05x_2 + 0.08x_3 - 0.03x_6 + 0.03x_7 \\ - 0.09x_9 - 0.01x_{10} - 0.07x_{11} + 0.25x_{13}^2 - 0.04x_{14} + 0.06x_{15} - 0.01x_{17} - 0.03x_{18},$$

over the design space  $[-0.5, 0.5]^{20}$ . The medium-fidelity code  $M_1$  is obtained by averaging  $H$  over a sliding window of size  $\pm\epsilon(x_l) = 0.1x_l$  over all 20 input dimensions. The low-fidelity codes  $L_1$  and  $L_2$  are similarly obtained by averaging  $M_1$  over a sliding window of size  $\pm\epsilon'(x_l) = 0.15x_l$  over 10 *odd* input dimensions (for  $L_1$ ) and 10 *even* dimensions (for  $L_2$ ). This provides three test functions which have nonlinear correlations with code  $H$ . The remaining medium-fidelity code  $M_2$  is then obtained via a simple approximation of  $H$ :  $Z_{M_2}(\mathbf{x}) = 1.2Z_H(\mathbf{x}) - 1$ .

To reflect the fact that higher-fidelity experiments are more expensive, we set the sample size for low- and medium-fidelity data at 200 and 160, respectively. The sample size for high-fidelity experiments is increased from 40 to 120 in increments of 20. The procedure in Section 4.1 is used for experimental design, using a maximin SLHD [1] with 14 slices and 20 samples per slice.

We compare the performance of the proposed d-GMGP model (trained using data at all five nodes) with three existing methods: a standard GP emulator trained using only data at  $H$ , the recursive KO model [5] and the nonlinear autoregressive multi-fidelity GP (NARGP) model [11]. Since the latter two methods can only account for multi-fidelity along a single path (i.e., from lowest to highest fidelity), these models are trained with data from the longest path in  $\mathcal{G}$ , namely,  $L_1$ ,  $M_1$  and  $H$ . The goal is to see whether the proposed model can leverage additional data on nodes  $L_2$  and  $M_2$  via the implicit DAG structure to provide improved predictive performance. All methods are tested on the same 500 randomly sampled points, and are compared on four metrics: (i) root-mean-squared-error (RMSE)  $\sqrt{n^{-1} \sum_{i=1}^n (\hat{y}_i - y_i)^2}$ , (ii) maximum absolute error (MAE)  $\max |\hat{y}_i - y_i|$ , (iii) root-integrated-predictive-variance (RIPV)  $\sqrt{n^{-1} \sum_{i=1}^n \text{var}(\hat{y}_i)}$ , and (iv) the probabilistic RMSE  $\sqrt{n^{-1} \sum_{i=1}^n [(\hat{y}_i - y_i)^2 + \text{var}(\hat{y}_i)]}$ . The procedure is repeated for 20 times to account for sampling variability.

Figure 3 shows the error boxplots of the four metrics for various high-fidelity sample sizes. There are several observations of interest. First, for all sample sizes, the proposed d-GMGP model outperforms existing models in terms of all four metrics. This shows that, by leveraging the underlying DAG structure used in

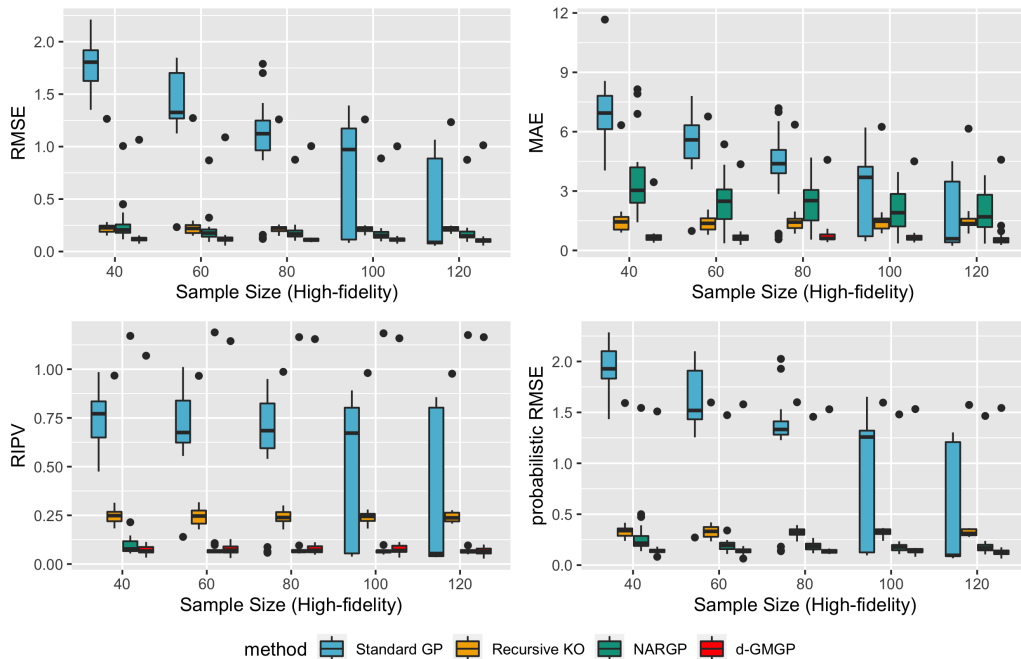


Figure 3: Error boxplots of the four metrics for different sample sizes on  $H$  (top-left: RMSE, top-right: MAE, bottom-left: RIPV, bottom-right: probabilistic RMSE).

the simulation model, the proposed method can yield significant improvements in terms of both predictive performance and uncertainty quantification. Second, this improvement seems to be most pronounced when the high-fidelity sample size is small. This is intuitive: as high-fidelity data becomes more limited (i.e., high-fidelity simulations become more expensive), additional structure linking multi-fidelity data should be more effective in improving predictive performance. Here, the deep GMGP model seems quite capable of leveraging this DAG structure for surrogate modeling, providing good predictive performance even in the challenging setting where high-fidelity data is limited in a high-dimensional input space.

## 6 Conclusion

In this paper, we presented a new Graphical Multi-fidelity Gaussian Process for surrogate modeling. The key novelty of the GMGP model is the use of a directed acyclic graph to model dependencies between computer codes. We showed that the GMGP has several appealing properties for multi-fidelity modeling, and presented several extensions which allow for nonlinear modeling and scalable prediction via recursive computation on sub-graphs. Numerical experiments confirm the improvement of the proposed method over existing methods, particularly when the amount of high-fidelity data is limited.

## References

- [1] S. Ba, W. R. Myers, and W. A. Breneman. Optimal Sliced Latin Hypercube Designs. *Technometrics*, 57(4):479–487, 2015.
- [2] K. Cutajar, M. Pullin, A. Damianou, N. Lawrence, and J. González. Deep Gaussian Processes for Multi-fidelity Modeling. *ArXiv*, abs/1903.07320, 2019.

- [3] A. Damianou and N. D. Lawrence. Deep Gaussian Processes. In C. M. Carvalho and P. Ravikumar, editors, *Proceedings of the Sixteenth International Conference on Artificial Intelligence and Statistics*, volume 31 of *Proceedings of Machine Learning Research*, pages 207–215, Scottsdale, Arizona, USA, 29 Apr–01 May 2013. PMLR.
- [4] D. Everett, W. Ke, J.-F. Paquet, G. Vujanovic, S. A. Bass, L. Du, C. Gale, M. Heffernan, U. Heinz, D. Liyanage, et al. Multisystem Bayesian constraints on the transport coefficients of QCD matter. *Physical Review C*, 103(5):054904, 2021.
- [5] L. L. Gratiet and J. Garnier. Recursive co-kriging model for Design of Computer experiments with multiple levels of fidelity. *International Journal for Uncertainty Quantification*, 4(5):365–386, 2014.
- [6] J. L. Gross, J. Yellen, and P. Zhang. *Handbook of Graph Theory, Second Edition*. Chapman & Hall/CRC, 2nd edition, 2013.
- [7] C. G. Kaufman, D. Bingham, S. Habib, K. Heitmann, J. A. Frieman, et al. Efficient emulators of computer experiments using compactly supported correlation functions, with an application to cosmology. *The Annals of Applied Statistics*, 5(4):2470–2492, 2011.
- [8] M. C. Kennedy and A. O’Hagan. Predicting the Output from a Complex Computer Code When Fast Approximations Are Available. *Biometrika*, 87(1):1–13, 2000.
- [9] S. Mak, C.-L. Sung, X. Wang, S.-T. Yeh, Y.-H. Chang, V. R. Joseph, V. Yang, and C. F. J. Wu. An efficient surrogate model for emulation and physics extraction of large eddy simulations. *Journal of the American Statistical Association*, 113(524):1443–1456, 2018.
- [10] A. O’Hagan. A Markov Property for Covariance Structures, 1998.
- [11] P. Perdikaris, M. Raissi, A. Damianou, N. D. Lawrence, and G. E. Karniadakis. Nonlinear information fusion algorithms for data-efficient multi-fidelity modelling. *Proceedings of the Royal Society A: Mathematical, Physical and Engineering Sciences*, 473(2198):20160751, feb 2017.
- [12] T. J. Santner, B. J. Williams, and W. I. Notz. *The Design and Analysis of Computer Experiments*, volume 1. Springer, 2003.
- [13] W. J. Welch, R. J. Buck, J. Sacks, H. P. Wynn, T. J. Mitchell, and M. D. Morris. Screening, Predicting, and Computer Experiments. *Technometrics*, 34(1):15–25, 1992.